EPJ A
Hadrons and Nuclei
EPJ.org
your physics journal

Eur. Phys. J. A (2018) **54**: 22 DOI 10.1140/epja/i2018-12424-7

Non-perturbative RPA-method implemented in the Coulomb gauge QCD Hamiltonian: From quarks and gluons to baryons and mesons

Tochtli Yepez-Martinez, Osvaldo Civitarese and Peter O. Hess

Società Italiana di Fisica
Springer

Eur. Phys. J. A (2018) **54**: 22
DOI 10.1140/epja/i2018-12424-7

THE EUROPEAN PHYSICAL JOURNAL A

Regular Article – Theoretical Physics

Non-perturbative RPA-method implemented in the Coulomb gauge QCD Hamiltonian: From quarks and gluons to baryons and mesons*

Tochtli Yepez-Martinez[1,a], Osvaldo Civitarese[1,b], and Peter O. Hess[2,3,c]

[1] Departamento de Fisica, Universidad Nacional de La Plata, C.C.67 (1900), La Plata, Argentina
[2] Instituto de Ciencias Nucleares, Universidad Nacional Autónoma de México, Ciudad Universitaria, Circuito Exterior S/N, A.P. 70-543, 04510 México D.F., Mexico
[3] Frankfurt Institute for Advanced Studies, Johann Wolfgang Goethe Universität, Ruth-Moufang-Str.1, 60438 Frankfurt am Main, Germany

Received: 25 August 2017 / Revised: 24 October 2017
Published online: 19 February 2018 –
Communicated by T. Biro

Abstract. Starting from an algebraic model based on the QCD-Hamiltonian and previously applied to study meson states, we have developed an extension of it in order to explore the structure of baryon states. In developing our approach we have adapted concepts taken from group theory and non-perturbative many-body methods to describe states built from effective quarks and anti-quarks degrees of freedom. As a Hamiltonian we have used the QCD Hamiltonian written in the Coulomb Gauge, and expressed it in terms of effective quark-antiquark, di-quarks and di-antiquark excitations. To gain some insights about the relevant interactions of quarks in hadronic states, the Hamiltonian was approximately diagonalized by mapping quark-antiquark pairs and di-quarks (di-antiquarks) onto phonon states. In dealing with the structure of the vacuum of the theory, color-scalar and color-vector states are introduced to account for ground-state correlations. While the use of a purely color-scalar ground state is an obvious choice, so that colorless hadrons contain at least three quarks, the presence of coupled color-vector pairs in the ground state allows for colorless excitations resulting from the action of color objects upon it.

1 Introduction

The identification of effective degrees of freedom and their interactions, a crucial step for the description of physical systems, has been the guide for several decades of exploration of the complexity of the quantum many-body problem. It has achieved remarkable success in a broad range of phenomena, from solid-state to nuclear and hadron physics. A great part of the suitable techniques has been discussed in Walter Greiner's text books. Here, we shall show that some of these techniques can also be applied to the until now unsolved regime of low-energy QCD. The results are quite encouraging and they are in many respects analogous to the results found in the nuclear-structure problem, where the identification of single-particle and hole excitations and collective vibrational and rotational degrees of freedom allows for the construction of effective interactions which have proved to describe the main features of the nuclear spectrum. We have taken, in order to illustrate the method, low-energy baryon-like states and discussed their structure in terms of the various couplings allowed by the QCD Hamiltonian in the Coulomb Gauge.

Several features of the non-perturbative regime of QCD have been explored within the Coulomb gauge framework, *e.g.*, see ref. [1]. Among them, the variational solutions obtained for the gluon- and ghost-propagator have played an important role in order to provide the first insights about the confinement scenario in this formalism. The variational procedure implemented in the Yang-Mills sector, first with a Gaussian ansatz for the vacuum wave functional [2,3] and then extended to cubic and quartic terms, generates a better agreement with Lattice results for the gluon propagator [4]. The variational approach to Yang-Mills theory in Coulomb gauge has been extended to full QCD by including a wave functional of the Dirac vacuum of the quarks in the presence of the gauge field [5–7].

In [8], the chiral symmetry breaking has been explored in the excited baryon spectrum, within the Coulomb gauge QCD formalism. Such analysis has been performed in a controlled way in terms of the number of harmonic

* Contribution to the Topical Issue "Frontiers in Nuclear, Heavy Ion and Strong Field Physics" edited by Tamás S. Biró, Carsten Greiner, Berndt Müller, Johann Rafelski, Horst Stöcker.

[a] e-mail: yepez@fisica.unlp.edu.ar
[b] e-mail: osvaldo.civitarese@fisica.unlp.edu.ar
[c] e-mail: hess@nucleares.unam.mx

oscillator shells, similar to that performed in [9], but also in terms of angular excitations of the Nucleon and Δ states with spin up to $J = 13/2$.

Also there has been an increasing effort from Lattice calculations [10,11] for a better understanding of the low-lying baryon states, including excited states. Although a faithful description of the baryon spectrum seems to be promising, there are some aspects that still have to be clarified, *e.g.* the identification of the Roper resonance. The Dyson-Schwinger equations (DSEs) have also provided with several insights about the baryon spectrum [12], as well as a few excited states, among them the Roper resonance [13,14]. In ref. [15], a complete review of baryon states is presented via Dyson-Schwinger and Bethe-Salpeter equations, as well as the relation between them and the Lattice QCD results.

Our present description is based on the use of effective quark and antiquark states and quark-antiquark, diquarks and di-antiquarks pairs and their interactions. The main steps of the method which we are going to present are the following: i) starting from the QCD Hamiltonian written in the Coulomb Gauge [2,3] we perform a diagonalization of the kinetic energy term to get quark and anti-quark states, ii) with these (generally speaking) single-quark states we re-write the color-charge density interactions (*e.g.* the Fadeev term of the Hamiltonian) and replace the interactions with gluons by a static potential $V(r) = (-\alpha/r) + (\beta r)$ [9], iii) a further diagonalization of the pair-like terms of the Hamiltonian is performed by applying the Random Phase Approximation [16], and finally, iv) the remaining terms of the Hamiltonian are treated as a generalized phonon-single-particle- and pair-interactions, keeping in all cases the symmetries of the QCD degrees of freedom at the level of meson and baryon-like states. Our main conjecture consists in the use of coloured-pair configurations of both quarks and antiquarks, in addition to the colorless quark-antiquark pair configurations, to construct baryon-like states by coupling these configurations to quarks or antiquarks. The formalism and general aspects of the model are described in sects. 2-4 and the application of it is illustrated in sect. 5. The conclusions are drawn in sect. 6.

2 From QCD to effective degrees of freedom

2.1 QCD Hamiltonian in the Coulomb gauge

We start from the QCD Hamiltonian in its canonical Coulomb gauge representation [17,18],

$$\begin{aligned}\boldsymbol{H}^{QCD} = \int \Big\{ & \frac{1}{2}\left[\mathcal{J}^{-1}\boldsymbol{\Pi}^{tr}\cdot\mathcal{J}\boldsymbol{\Pi}^{tr} + \mathcal{B}\cdot\mathcal{B}\right] \\ & -\overline{\psi}\left(-i\gamma\cdot\nabla + m\right)\psi - g\overline{\psi}\gamma\cdot A\psi\Big\}\mathrm{d}\mathbf{x} \\ & + \frac{g^2}{2}\int \mathcal{J}^{-1}\rho^c(\mathbf{x})\langle c,\mathbf{x}|\frac{1}{\nabla\cdot\mathcal{D}}(-\nabla^2)\frac{1}{\nabla\cdot\mathcal{D}}|c'\mathbf{y}\rangle \\ & \times\mathcal{J}\rho^{c'}(\mathbf{y})\mathrm{d}\mathbf{x}\,\mathrm{d}\mathbf{y}, \end{aligned} \tag{1}$$

which has been widely studied in the past [2–9,19–23] for the description of characteristic features of QCD in its non-perturbative regime, like the confinement of color-charged particles along with the constituent quark and gluon masses. The structure of several bound states predicted by the theory has been described extensively [8,19–21,24–26]. A complete description of the Hamiltonian can be found in refs. [2,3,17]. Here, we just add a few comments to the already published material. The Hamiltonian of eq. (1) takes into account the interactions between quarks and gluons through the QCD *Instantaneous color-Coulomb Interaction* (QCD-IcCI) between color-charge densities of quarks and gluons. At low energy the effects of dynamical gluons in the QCD-IcCI are accounted for by the interaction $V(|\mathbf{x}-\mathbf{y}|) = -\frac{\alpha}{|\mathbf{x}-\mathbf{y}|} + \beta|\mathbf{x}-\mathbf{y}|$, which is obtained from a self-consistent treatment of the last term of the Hamiltonian [2,3].

In [9], the Hamiltonian of eq. (1) was written by keeping the quark-sector and using the effective confining interaction $V(|\mathbf{x}-\mathbf{y}|)$, namely

$$\begin{aligned}\boldsymbol{H}^{QCD}_{eff} = & \int\left\{\boldsymbol{\psi}^\dagger(\mathbf{x})(-i\boldsymbol{\alpha}\cdot\boldsymbol{\nabla} + \beta m)\boldsymbol{\psi}(\mathbf{x})\right\}\mathrm{d}\mathbf{x} \\ & -\frac{1}{2}\int\rho_c(\mathbf{x})V(|\mathbf{x}-\mathbf{y}|)\rho^c(\mathbf{y})\mathrm{d}\mathbf{x}\,\mathrm{d}\mathbf{y} \\ & = \boldsymbol{K} + \boldsymbol{H}_{\mathrm{Coul}}, \end{aligned} \tag{2}$$

where $\rho^c(\mathbf{x}) = \psi^\dagger(\mathbf{x})T^c\psi(\mathbf{x})$ is the quark and antiquark color-charge density. In eq. (2), the first term is the kinetic energy, while the second term is the QCD-IcCI in its simplified form. The fermion field $\psi^\dagger(\mathbf{x})$, whose quantization is explained in [9], is expanded in terms of creation and annihilation operators of particles (antiparticles) in a basis of harmonic-oscillator functions.

The use of the harmonic-oscillator basis (Nl) requires a pre-diagonalization, which is performed by means of a unitary transformation between creation (annihilation) operators in the harmonic-oscillator basis $\boldsymbol{q}^\dagger_{\tau(Nl)}(\boldsymbol{q}^{\tau(Nl)})$ and those belonging to an effective basis $\boldsymbol{Q}^\dagger_{\lambda k\pi_q}(\boldsymbol{Q}^{\lambda k\pi_q})$ of quarks (antiquarks), such that

$$\begin{aligned}\boldsymbol{q}^\dagger_{\tau(Nl)J_qC_q(Y_q,T_q),M_{J_q}M_{C_q}M_{T_q}} = & \sum_{\lambda\pi_q k}\left(\alpha^{J_q,T_q}_{\tau(Nl),\lambda\pi_q k}\right)^* \\ \times\boldsymbol{Q}^\dagger_{\lambda k\pi_q J_qC_q(Y_q,T_q),M_{J_q}M_{C_q}M_{T_q}}&\delta_{\pi_q,(-1)^{\frac{1}{2}-\tau+l}}. \end{aligned} \tag{3}$$

The effective quark $\boldsymbol{b}^\dagger$ and antiquark $\boldsymbol{d}$ operators are obtained via

$$\begin{aligned}&\boldsymbol{Q}^\dagger_{\frac{1}{2}k\pi_qJ_qC_q(Y_q,T_q),M_{J_q}M_{C_q}M_{T_q}} \\ &= \boldsymbol{b}^\dagger_{k\pi_qJ_qC_q(Y_q,T_q),M_{J_q}M_{C_q}M_{T_q}}. \end{aligned} \tag{4}$$

and

$$\begin{aligned}&\boldsymbol{Q}^\dagger_{-\frac{1}{2}k\pi_qJ_qC_q(Y_q,T_q),M_{J_q}M_{C_q}M_{T_q}} \\ &= \boldsymbol{d}_{k\pi_qJ_qC_q(Y_q,T_q),M_{J_q}M_{C_q}M_{T_q}}. \end{aligned} \tag{5}$$

The sub-index $\pi_q = \pm$ indicates the parity of the effective quark or antiquark and $k = 1, 2, \cdots$ runs over all

Table 1. Short-hand notation for the representation of the vacuum, quark, *ph*-pair, di-q and di-$\bar{q}$ irreps.

Representation	$\gamma_n = \{J_n, C_n, (Y_n, T_n)\}$	J_n	C_n	(Y_n, T_n)
vacuum (0)	$\gamma_0 = \{J_0, C_0, (Y_0, T_0)\}$	0	(00)	$(0,0)$
quark (q)	$\gamma_q = \{J_q, C_q, (Y_q, T_q)\}$	$\frac{1}{2}$	(10)	$\left(\frac{1}{3}, \frac{1}{2}\right)$, $\left(-\frac{2}{3}, 0\right)$
ph-pair (p)	$\gamma_p = \{J_p, C_p, (Y_p, T_p)\}$	0, 1	(00), (11)	$(0,0)$, $(0,1)$, $\left(\pm 1, \frac{1}{2}\right)$
di-q (a)	$\gamma_a = \{J_a, C_a, (Y_a, T_a)\}$	0, 1	(20), (01)	$\left(\frac{2}{3}, 1\right)$, $\left(\frac{2}{3}, 0\right)$, $\left(-\frac{1}{3}, \frac{1}{2}\right)$, $\left(-\frac{4}{3}, 0\right)$
di-$\bar{q}$ (r)	$\gamma_r = \{J_r, C_r, (Y_r, T_r)\}$	0, 1	(02), (10)	$\left(-\frac{2}{3}, 1\right)$, $\left(-\frac{2}{3}, 0\right)$, $\left(\frac{1}{3}, \frac{1}{2}\right)$, $\left(\frac{4}{3}, 0\right)$

orbital states. As in [9] we shall label the states by the hypercharge, isospin and third component of isospin. The index $J_q = \frac{1}{2}, \frac{3}{2}, \cdots$ indicates the total ($J_q = l \pm \frac{1}{2}$) single-particle spin. The flavor hypercharge and isospin quantum numbers for quarks are given by $(Y_q, T_q) = (\frac{1}{3}, \frac{1}{2}), (-\frac{2}{3}, 0)$. The quarks and antiquarks belong to a triplet $C_q = (10)$ and antitriplet $\bar{C}_q = C_{\bar{q}} = (01)$ color irreducible representations (irreps), respectively, which are conjugate representations. In order to reduce the number of indices, we will use the short-hand notation $\gamma_q = \{J_q, C_q, (Y_q, T_q)\}$ for the quarks and $\bar{\gamma}_q = \{J_q, \bar{C}_q, (\bar{Y}_q, T_q)\}$ for antiquarks irreps with $\bar{Y}_q = -Y_q$, while $\mu_q = \{M_{J_q}, M_{C_q}, M_{T_q}\}$ and $\bar{\mu}_q = \{\bar{M}_{J_q}, \bar{M}_{C_q}, \bar{M}_{T_q}\}$ will be used for the magnetic numbers with $\bar{M}_{J_q} = -M_{J_q}$ and $\bar{M}_{T_q} = -M_{T_q}$.

The kinetic ($\boldsymbol{K}$) term rewritten in terms of effective quarks and antiquarks operators has the following structure [9,21]:

$$\boldsymbol{K} = \sum_{k\pi_q\gamma_q} \varepsilon_{k\pi_q\gamma_q} \sum_{\mu_q} \left(\boldsymbol{b}^{\dagger}_{k\pi_q,\gamma_q\mu_q} \boldsymbol{b}^{k\pi_q,\gamma_q\mu_q} - \boldsymbol{d}^{k\pi_q,\bar{\gamma}_q\bar{\mu}_q} \boldsymbol{d}^{\dagger}_{k\pi_q,\bar{\gamma}_q\bar{\mu}_q} \right), \tag{6}$$

where the rules to raise and lower indices are taken from [9, 27] and they are listed in the appendix A.

The QCD-IcCI term, in its simplified form ($\boldsymbol{H}_{\rm Coul}$), rewritten in terms of effective quark and antiquark operators is given by [9]

$$\begin{aligned} \boldsymbol{H}_{\rm Coul} = -\frac{1}{2} \sum_{L} \sum_{\lambda_i \mathbf{q}_i} V^{L}_{\{\lambda_i \mathbf{q}_i\}} \\ \times \Big(\left[\mathcal{F}_{\lambda_1\mathbf{q}_1,\lambda_2\mathbf{q}_2;\gamma_{f_0}} \mathcal{F}_{\lambda_3\mathbf{q}_3,\lambda_4\mathbf{q}_4;\bar{\gamma}_{f_0}} \right]^{\gamma_0}_{\mu_0} \\ + \left[\mathcal{F}_{\lambda_1\mathbf{q}_1,\lambda_2\mathbf{q}_2;\gamma_{f_0}} \mathcal{G}_{\lambda_3\mathbf{q}_3,\lambda_4\mathbf{q}_4;\bar{\gamma}_{f_0}} \right]^{\gamma_0}_{\mu_0} \\ + \left[\mathcal{G}_{\lambda_1\mathbf{q}_1,\lambda_2\mathbf{q}_2;\gamma_{f_0}} \mathcal{F}_{\lambda_3\mathbf{q}_3,\lambda_4\mathbf{q}_4;\bar{\gamma}_{f_0}} \right]^{\gamma_0}_{\mu_0} \\ + \left[\mathcal{G}_{\lambda_1\mathbf{q}_1,\lambda_2\mathbf{q}_2;\gamma_{f_0}} \mathcal{G}_{\lambda_3\mathbf{q}_3,\lambda_4\mathbf{q}_4;\bar{\gamma}_{f_0}} \right]^{\gamma_0}_{\mu_0} \Big), \end{aligned} \tag{7}$$

where we have compacted the single-particle orbital number, parity and irreps, into the short-hand notation $\mathbf{q}_i = k_i \pi_{q_i} \gamma_{q_i}$, and use for the (flavorless) quantum numbers of the intermediate coupling in the interaction the label $\gamma_{f_0} = \{L, (11), (0,0)\}$ and for their magnetic projections $\mu_{f_0} = \{M_L, M_C, 0\}$, respectively. The conjugate representations satisfy $\bar{\gamma}_{f_0} = \gamma_{f_0}$ and $\bar{\mu}_{f_0} = \{-M_L, \bar{M}_C, 0\}$. Then for the total couplings (upper index) and magnetic numbers (lower index) of the interaction, we have used $\gamma_0 = \{0, (00), (0,0)\}$ and $\mu_0 = \{0,0,0\}$ respectively. The operators $\mathcal{F}$ and $\mathcal{G}$ are written

$$\begin{aligned} \mathcal{F}_{\lambda_1\mathbf{q}_1,\lambda_2\mathbf{q}_2;\gamma_{f_0},\mu_{f_0}} = \frac{1}{\sqrt{2}} \Big\{ \delta_{\lambda_1,\frac{1}{2}} \delta_{\lambda_2,\frac{1}{2}} \left[\boldsymbol{b}^{\dagger}_{\mathbf{q}_1} \otimes \boldsymbol{b}_{\bar{\mathbf{q}}_2} \right]^{\gamma_{f_0}}_{\mu_{f_0}} \\ - \delta_{\lambda_1,-\frac{1}{2}} \delta_{\lambda_2,-\frac{1}{2}} \left[\boldsymbol{d}_{\bar{\mathbf{q}}_1} \otimes \boldsymbol{d}^{\dagger}_{\bar{\mathbf{q}}_2} \right]^{\gamma_{f_0}}_{\mu_{f_0}} \Big\} \\ \mathcal{G}_{\lambda_1\mathbf{q}_1,\lambda_2\mathbf{q}_2;\gamma_{f_0},\mu_{f_0}} = \frac{1}{\sqrt{2}} \Big\{ \delta_{\lambda_1,-\frac{1}{2}} \delta_{\lambda_2,\frac{1}{2}} \left[\boldsymbol{d}_{\mathbf{q}_1} \otimes \boldsymbol{b}_{\bar{\mathbf{q}}_2} \right]^{\gamma_{f_0}}_{\mu_{f_0}} \\ - \delta_{\lambda_1,\frac{1}{2}} \delta_{\lambda_2,-\frac{1}{2}} \left[\boldsymbol{b}^{\dagger}_{\mathbf{q}_1} \otimes \boldsymbol{d}^{\dagger}_{\bar{\mathbf{q}}_2} \right]^{\gamma_{f_0}}_{\mu_{f_0}} \Big\}. \end{aligned} \tag{8}$$

The Hamiltonian expressed in the effective quark and antiquark operators, eqs. (6) and (7), describes bound states (mesons and baryons) of these effective particles. In [9] the low-energy mesons states with $J^{\pi} = 0^{\pm}, 1^{-}$ were represented by particle(quarks)-hole(antiquarks) (or *ph*) phonons by means of the *Tamm-Dancoff-Approximation* and the *Random-Phase-Approximation* methods. Those methods provide some insights about the low-energy meson spectrum and the influence of *ph*-correlations in the vacuum. As we have mentioned before the *ph*-correlations are colorless in order to describe meson-states as one-phonon excitations of the vacuum. In the present work we go further and have considered color-correlations in a more general description of the vacuum. These color correlations, viewed as excitations of the vacuum, can not describe physical states but they may be coupled to color-vector configurations to describe bound states *e.g.*, baryon states, which are constructed such that the overall color is zero.

3 Representations and operators

In the previous section we have introduced the short-hand notation for quark- and antiquark-irreps γ_q and $\bar{\gamma}_q$, as well as their magnetic numbers μ_q and $\bar{\mu}_q$, noticing that $\gamma_{\bar{q}} = \bar{\gamma}_q$ and $\mu_{\bar{q}} = \bar{\mu}_q$. We have also introduced the compact notation $\mathbf{q}_i = k_i \pi_{q_i} \gamma_{q_i}$. The representations corresponding to the vacuum, meson-like (or *ph*-pair), di-quarks (di-q) and di-antiquarks (di-$\bar{q}$) states are introduced in table 1, where a similar short-hand notation $\gamma_n = \{J_n, C_n, (Y_n, T_n)\}$ is

used. The sub-index $n = 0, q, p, a, r$ reads for the vacuum, quarks, mesons, di-quarks and di-antiquarks states, respectively. In this work we only consider quarks and antiquarks with total spin $J_q = \frac{1}{2}$.

For the baryon state representations and magnetic components we will use $\gamma_{B_i} = \{J_{B_i}, C_{B_i}, (Y_{B_i} T_{B_i})\}$ and $\mu_{B_i} = \{M_{J_{B_i}}, M_{C_{B_i}}, M_{(Y_{B_i}, T_{B_i})}\}$, respectively, and focus on specific physical representations (see sect. 3.4).

3.1 Vacuum state and operators

In [9] the correlated vacuum which includes *ph* correlations was constructed explicitly using the RPA formalism. The RPA solutions aimed to describe meson-like states, so that the *ph*-pairs responsible for ground-state correlations were (00)-colorless configurations. In general, the ground state can include also color correlations by means of colored (11)-*ph*-pairs and (20), (01)-di-q and (02), (10)-di-$\bar{q}$ operators. Up to second order in the quark-antiquarks operators, we can relate the new ground state to the vacuum state $|\tilde{0}\rangle$ via

$$
\begin{aligned}
|RPA\rangle = |\tilde{0}\rangle & \\
&+ \sum_{p\pi_p;\gamma_p} \sum_{\mathbf{q}_i'\mathbf{q}_i} Z^{p\pi_p,\gamma_p}_{(1)\,\mathbf{q}_1'\bar{\mathbf{q}}_2',\mathbf{q}_1\bar{\mathbf{q}}_2} \\
&\times \left[\left[\boldsymbol{b}^\dagger_{\mathbf{q}_1'} \otimes \boldsymbol{d}^\dagger_{\bar{\mathbf{q}}_2'} \right]^{\gamma_p} \otimes \left[\boldsymbol{b}^\dagger_{\mathbf{q}_1} \otimes \boldsymbol{d}^\dagger_{\bar{\mathbf{q}}_2} \right]^{\bar{\gamma}_p} \right]^{\gamma_0}_{\mu_0} |\tilde{0}\rangle \\
&+ \sum_{a\pi_a;\gamma_a} \sum_{\mathbf{q}_i'\mathbf{q}_i} Z^{a\pi_a,\gamma_a}_{(2)\,\mathbf{q}_1'\mathbf{q}_2',\bar{\mathbf{q}}_1\bar{\mathbf{q}}_2} \\
&\times \left[\left[\boldsymbol{b}^\dagger_{\mathbf{q}_1'} \otimes \boldsymbol{b}^\dagger_{\mathbf{q}_2'} \right]^{\gamma_a} \otimes \left[\boldsymbol{d}^\dagger_{\bar{\mathbf{q}}_1'} \otimes \boldsymbol{d}^\dagger_{\bar{\mathbf{q}}_2'} \right]^{\bar{\gamma}_a} \right]^{\gamma_0}_{\mu_0} |\tilde{0}\rangle. \quad (9)
\end{aligned}
$$

The $Z^{p\pi_p,\gamma_p}_{(1)\,\mathbf{q}_1'\bar{\mathbf{q}}_2',\mathbf{q}_1\bar{\mathbf{q}}_2}$ and the $Z^{a\pi_a,\gamma_a}_{(2)\,\mathbf{q}_1'\mathbf{q}_2',\bar{\mathbf{q}}_1\bar{\mathbf{q}}_2}$ vacuum contributions can be related by re-couplings in spin, color and flavor quantum numbers. However we prefer to show explicitly the *ph*-pair and di-q–di-$\bar{q}$ correlations and take into account the corresponding re-couplings in the effective Hamiltonian once the RPA dynamical equation of motion, eq. (22), is implemented for the different sub-spaces of diagonalization. This is explained in sect. 4. The vacuum coefficients $Z^{n\pi_n,\gamma_n}_{(i)\,\mathbf{q}_1'\mathbf{q}_2',\mathbf{q}_1\mathbf{q}_2}$ satisfy a similar relation in terms of the forward $X_{\mathbf{q}_1\mathbf{q}_2;n\pi_n\gamma_n}$ and backward $Y_{\mathbf{q}_1'\mathbf{q}_2';n\pi_n\gamma_n}$ amplitudes namely

$$
Z^{n\pi_n,\gamma_n}_{\mathbf{q}_1'\mathbf{q}_2',\mathbf{q}_1\mathbf{q}_2} = \sqrt{\dim(\gamma_n)} Y_{\mathbf{q}_1'\mathbf{q}_2';n\pi_n\gamma_n} \left(X_{\mathbf{q}_1\mathbf{q}_2;n\pi_n\gamma_n}\right)^{-1}, \quad (10)
$$

see sect. 3.3. In a schematic representation the vacuum can be depicted as

$$
|RPA\rangle = |\tilde{0}\rangle + Z_{(1)} |\,[\uparrow\downarrow]^\dagger\,[\uparrow\downarrow]^\dagger\rangle + Z_{(2)} |\,[\uparrow\uparrow]^\dagger\,[\downarrow\downarrow]^\dagger\rangle \quad (11)
$$

with $[\uparrow\downarrow]$ representing *ph*-pairs and $[\uparrow\uparrow]([\downarrow\downarrow])$ representing colored di-q(di-$\bar{q}$) ones.

3.2 ph, di-quark and di-antiquark operators

The *ph*-pair operators (or quark-antiquark operators) can be expressed in their decoupled form as

$$
\begin{aligned}
&\left[\boldsymbol{b}^\dagger_{\mathbf{q}_1} \otimes \boldsymbol{d}^\dagger_{\bar{\mathbf{q}}_2} \right]^{\gamma_p}_{\mu_p} = \\
&\sum_{M_{J_{q_i}} M_{C_{q_i}} M_{T_{q_i}}} \langle J_{q_1} M_{J_{q_1}}, J_{q_2} \bar{M}_{J_{q_2}} | J_p M_{J_p} \rangle \\
&\langle (10) M_{C_{q_1}}, (01) \bar{M}_{C_{q_2}} | C_p M_{C_p} \rangle \langle T_{q_1} M_{T_{q_1}}, T_{q_2} \bar{M}_{T_{q_2}} | T_p M_{T_p} \rangle \\
&\boldsymbol{b}^\dagger_{k_1,\pi_{q_1},J_{q_1}(10)(Y_{q_1},T_{q_1});M_{J_{q_1}} M_{C_{q_1}} M_{T_{q_1}}} \\
&\boldsymbol{d}^\dagger_{k_2,\pi_{q_2},J_{q_2}(01)(\bar{Y}_{q_2},T_{q_2});\bar{M}_{J_{q_2}} \bar{M}_{C_{q_2}} \bar{M}_{T_{q_2}}} \delta_{\pi_p,\pi_{q_1}\pi_{q_2}}. \quad (12)
\end{aligned}
$$

The *ph*-pair color representations $C_p = (00)$ may be directly related to physical states while the colored $C_p = (11)$ ones need another operator in order to couple to a colorless representation.

The di-q operators are given by

$$
\begin{aligned}
&\left[\boldsymbol{b}^\dagger_{\mathbf{q}_1} \otimes \boldsymbol{b}^\dagger_{\mathbf{q}_2} \right]^{\gamma_a}_{\mu_a} = \\
&\sum_{M_{J_{q_i}} M_{C_{q_i}} M_{T_{q_i}}} \langle J_{q_1} M_{J_{q_1}}, J_{q_2} M_{J_{q_2}} | J_a M_{J_a} \rangle \\
&\langle (10) M_{C_{q_1}}, (10) M_{C_{q_2}} | C_a M_{C_a} \rangle \langle T_{q_1} M_{T_{q_1}}, T_{q_2} M_{T_{q_2}} | T_a M_{T_a} \rangle \\
&\boldsymbol{b}^\dagger_{k_1,\pi_{q_1},J_{q_1}(10)(Y_{q_1},T_{q_1});M_{J_{q_1}} M_{C_{q_1}} M_{T_{q_1}}} \\
&\boldsymbol{b}^\dagger_{k_2,\pi_{q_2},J_{q_2}(10)(Y_{q_2},T_{q_2});M_{J_{q_2}} M_{C_{q_2}} M_{T_{q_2}}} \delta_{\pi_a,\pi_{q_1}\pi_{q_2}}. \quad (13)
\end{aligned}
$$

The di-antiquarks operator are given by

$$
\begin{aligned}
&\left[\boldsymbol{d}^\dagger_{\bar{\mathbf{q}}_1} \otimes \boldsymbol{d}^\dagger_{\bar{\mathbf{q}}_2} \right]^{\gamma_r}_{\mu_r} = \\
&\sum_{M_{J_{q_i}} M_{C_{q_i}} M_{T_{q_i}}} \langle J_{q_1} \bar{M}_{J_{q_1}}, J_{q_2} \bar{M}_{J_{q_2}} | J_r M_{J_r} \rangle \\
&\langle (01) \bar{M}_{C_{q_1}}, (01) \bar{M}_{C_{q_2}} | C_r M_{C_r} \rangle \langle T_{q_1} \bar{M}_{T_{q_1}}, T_{q_2} \bar{M}_{T_{q_2}} | T_r M_{T_r} \rangle \\
&\boldsymbol{d}^\dagger_{k_1,\pi_{q_1},J_{q_1}(01)(\bar{Y}_{q_1},T_{q_1});\bar{M}_{J_{q_1}} \bar{M}_{C_{q_1}} \bar{M}_{T_{q_1}}} \\
&\boldsymbol{d}^\dagger_{k_2,\pi_{q_2},J_{q_2}(01)(\bar{Y}_{q_2},T_{q_2});\bar{M}_{J_{q_2}} \bar{M}_{C_{q_2}} \bar{M}_{T_{q_2}}} \delta_{\pi_r,\pi_{q_1}\pi_{q_2}}. \quad (14)
\end{aligned}
$$

Clearly the di-q(di-$\bar{q}$) are colored operators and they need for another colored operator, *e.g.* a quark(antiquark) operator, to couple to a colorless object to describe physical states.

3.3 ph-, di-quark- and di-antiquark phonon operators

The effective QCD Hamiltonian, eq. (2), can be expressed in terms of the *ph*-pair, di-q and di-$\bar{q}$ operators introduced above. The one-phonon creation-operators of the

ph-, di-quark– and di-antiquark–type are defined

$$\boldsymbol{\Gamma}^{\dagger}_{p\pi_p\gamma_p\mu_p} = \sum_{\mathbf{q}_\alpha,\mathbf{q}_\beta} \Big\{ X_{\mathbf{q}_\alpha\mathbf{q}_\beta;p\pi_p\gamma_p} \left[\boldsymbol{b}^{\dagger}_{\mathbf{q}_\alpha} \otimes \boldsymbol{d}^{\dagger}_{\bar{\mathbf{q}}_\beta}\right]^{\gamma_p}_{\mu_p} - Y_{\mathbf{q}_\alpha\mathbf{q}_\beta;p\pi_p\gamma_p}(-1)^{\phi_{\gamma_p\mu_p}} \left[\boldsymbol{d}^{\bar{\mathbf{q}}_\beta} \otimes \boldsymbol{b}^{\mathbf{q}_\alpha}\right]^{\bar{\gamma}_p}_{\bar{\mu}_p} \Big\} \tag{15}$$

$$\boldsymbol{\Gamma}^{\dagger}_{a\pi_a,\gamma_a\mu_a} = \sum_{\mathbf{q}_\alpha,\mathbf{q}_\beta} \Big\{ X'_{\mathbf{q}_\alpha\mathbf{q}_\beta;a\pi_a\gamma_a} \left[\boldsymbol{b}^{\dagger}_{\mathbf{q}_\alpha} \otimes \boldsymbol{b}^{\dagger}_{\mathbf{q}_\beta}\right]^{\gamma_a}_{\mu_a} - Y'_{\mathbf{q}_\alpha\mathbf{q}_\beta;a\pi_a\gamma_a}(-1)^{\phi_{\gamma_a\mu_a}} \left[\boldsymbol{d}^{\bar{\mathbf{q}}_\beta} \otimes \boldsymbol{d}^{\bar{\mathbf{q}}_\alpha}\right]^{\bar{\gamma}_a}_{\bar{\mu}_a} \Big\} \tag{16}$$

and

$$\boldsymbol{\Gamma}^{\dagger}_{r\pi_r,\gamma_r\mu_r} = \sum_{\mathbf{q}_\alpha,\mathbf{q}_\beta} \Big\{ X''_{\mathbf{q}_\alpha\mathbf{q}_\beta;r\pi_r\gamma_r} \left[\boldsymbol{d}^{\dagger}_{\bar{\mathbf{q}}_\alpha} \otimes \boldsymbol{d}^{\dagger}_{\bar{\mathbf{q}}_\beta}\right]^{\gamma_r}_{\mu_r} - Y''_{\mathbf{q}_\alpha\mathbf{q}_\beta;r\pi_r\gamma_r}(-1)^{\phi_{\gamma_r\mu_r}} \left[\boldsymbol{b}^{\mathbf{q}_\beta} \otimes \boldsymbol{b}^{\mathbf{q}_\alpha}\right]^{\bar{\gamma}_r}_{\bar{\mu}_r} \Big\}, \tag{17}$$

respectively, where the amplitudes X and Y are the forward- and backward-going amplitudes. The phase $(-1)^{\phi_{\gamma_n\mu_n}} = (-1)^{J_n - M_{J_n}}(-1)^{\chi_{C_n}}(-1)^{T_n - M_{T_n}}$ in each phonon operator $n = p, a, r$ accounts for the scalar couplings in the vacuum, eq. (9).

The one-phonon annihilation operators $\boldsymbol{\Gamma}^{n\pi_n\gamma_n\mu_n} = (\boldsymbol{\Gamma}^{\dagger}_{n\pi_n,\gamma_n\mu_n})^{\dagger}$ satisfy $\Gamma^{n\pi_n\gamma_n\mu_n}|RPA\rangle = 0$, for $n = p, a, r$. Due to the fact that the di-q and di-$\bar{q}$ are conjugate representations, the determination of the vacuum amplitudes $Z^{n\pi_n,\gamma_n}_{(2)\,\mathbf{q}'_1\mathbf{q}'_2,\bar{\mathbf{q}}_1\bar{\mathbf{q}}_2}$ for the cases $n = a, r$, yields

$$Y'_{\mathbf{q}'_1\mathbf{q}'_2;a\pi_a\gamma_a}\left(X'_{\mathbf{q}_1\mathbf{q}_2;a\pi_a\gamma_a}\right)^{-1} = Y''_{\mathbf{q}'_1\mathbf{q}'_2;r\pi_r\gamma_r}\left(X''_{\mathbf{q}_1\mathbf{q}_2;r\pi_r\gamma_r}\right)^{-1}, \tag{18}$$

which is needed for the inversion of the transformation of eqs. (16) and (17), as well as for the mapping of H^{QCD}_{eff} onto the RPA basis (sect. 4).

3.4 Baryon-like operators and representations

To complete this section we shall now introduce the baryon representation obtained from the effective quarks and the phonon operators described above. The present work focuses on the description of the low-energy baryon p, n and Δ states. Therefore, we will focus on the quantum numbers $T_B(J^{\pi_B}_B) = \frac{1}{2}(\frac{1}{2}^+)$, $\frac{3}{2}(\frac{3}{2}^+)$ and $C_B = (00)$, in order to describe such baryon-like states. For both baryon flavor-isospin values $T_B = \frac{1}{2}$ and $\frac{3}{2}$, the flavor-hypercharge is equal to $Y_B = 1$.

The simplest baryon-like operators in this scheme are given by

$$\boldsymbol{B}^{\dagger}_{B_1\pi_{B_1},\gamma_{B_1}\mu_{B_1}} = \left[\boldsymbol{b}^{\dagger}_{\mathbf{q}_1} \otimes \boldsymbol{b}^{\dagger}_{\mathbf{q}_2} \otimes \boldsymbol{b}^{\dagger}_{\mathbf{q}_3}\right]^{\gamma_{B_1}}_{\mu_{B_1}}, \tag{19}$$

where $\pi_{B_1} = \prod_i \pi_{q_i}$ and $\gamma_{B_1} = \{J_{B_1}, (Y_{B_1}T_{B_1}), C_{B_1}\}$. These baryon-like operators do not account for any ground-state correlations.

The first baryon-like operators that account for ground-state correlations are

$$\boldsymbol{B}^{\dagger}_{B_2\pi_{B_2},\gamma_{B_2}\mu_{B_2}} = \left[\boldsymbol{B}^{\dagger}_{B_1\pi_{B_1},\gamma_{B_1}} \otimes \boldsymbol{\Gamma}^{\dagger}_{p\pi_p,\gamma_p}\right]^{\gamma_{B_2}}_{\mu_{B_2}}. \tag{20}$$

The number of baryon-like representations for the $\boldsymbol{B}^{\dagger}_{B_2}$ operator is vast and they are obtained by the coupling of the irreps of the colorless *ph*-phonon states (3.2) and those of the baryon-like configurations of three quarks, as in eq. (19).

As we have mentioned, for the purpose of the present work we focus on the baryon-like irreps related to the nucleon and Δ states, *i.e.*, $J^{\pi_{B_2}}_{B_2} = \frac{1}{2}^+$ and $\frac{3}{2}^+$, $(Y_{B_2}T_{B_2}) = (1, \frac{1}{2})$ and $(1, \frac{3}{2})$ and $C_{B_2} = (00)$.

In order to get a positive parity for such baryon-like states we take the lowest-energy meson-like solution of the RPA spectrum. It turns out that such phonon has the quantum numbers of the pion state, see sect. 4, which requires for the baryon like operators $\boldsymbol{B}^{\dagger}_{B_1\pi_{B_1},\gamma_{B_1}}$, in eq. (20), to have negative parity $J^{\pi_{B_1}}_{B_1} = \frac{1}{2}^-, \frac{3}{2}^-$.

The other baryon-like operator that accounts for ground-state correlations is

$$\boldsymbol{B}^{\dagger}_{B_3\pi_{B_3},\gamma_{B_3}\mu_{B_3}} = \left[\left[\boldsymbol{b}^{\dagger}_{\mathbf{q}_1} \otimes \left[\boldsymbol{b}^{\dagger}_{\mathbf{q}_2} \otimes \boldsymbol{d}^{\dagger}_{\bar{\mathbf{q}}_3}\right]^{\gamma_0}\right]_{\mathbf{q}_1} \otimes \boldsymbol{\Gamma}^{\dagger}_{a,\pi_a\gamma_a}\right]^{\gamma_{B_3}}_{\mu_{B_3}}, \tag{21}$$

where this operator can be seen as a quark in the presence of a simple scalar *ph*-pair and a di-quark phonon. In order to describe a positive-parity baryon-like state, the quark denoted by $\mathbf{q}_1$ has the same parity as the di-q phonon operator $\pi_{q_1} = \pi_a$. For the present work, we only consider the di-q phonon state $T_a(J^{\pi}_a) = 0(0^+)$, which corresponds to the lowest RPA solutions within the $SU(3)$ color subspace (01), needed in order to satisfy the colorless condition of a physical state.

Under this approximation, the baryon-like operator (21) contributes to proton (neutron)-like states and not to Δ-like states. This provides a description for the Δ-like state minimally as a combination of a pure three-quarks state and a baryon-meson bound state. The solutions for the lowest *ph*-pair and di-q phonon-states are shown in sect. 5.

4 Bosonizations and the Hamiltonian

The RPA method is used to map the effective QCD Hamiltonian (2) onto a Hamiltonian describing the propagation of quarks, antiquarks and *ph*-, di-q-, di-$\bar{q}$-phonons as well as their interactions. The equation of motion in the RPA formalism ($\boldsymbol{H}^{QCD}_{eff}|n\pi_n\gamma_n\mu_n\rangle = \omega_{n\pi_n\gamma_n}|n\pi_n\gamma_n\mu_n\rangle$) is equivalent to the double commutator

$$\langle RPA|\left[\hat{I}^{n'\pi_n\gamma_n\mu_n}, \left[\boldsymbol{H}^{QCD}_{eff}, I^{\dagger}_{n\pi_n\gamma_n\mu_n}\right]\right]|RPA\rangle = \omega_{n\pi_n\gamma_n}\delta_{n,n'}, \tag{22}$$

with eigenvalues $\omega_{n\pi_n\gamma_n}$ for $n = p, a, r$. The latter implies four color subspaces of diagonalization *i.e.*, $C_p = (00), (11)$

and $C_a = (20), (01)$, since the corresponding diagonalizations in the subspaces $C_r = (02)$ and $C_r = (10)$ are symmetric with respect to $C_a = (20)$ and $C_a = (01)$, respectively. In a first stage the RPA method leaves out the Hamiltonian terms H_{31} and H_{13}, *i.e.* the second and third terms in eq. (7), corresponding to three creation and one annihilation operators and their Hermitian conjugate terms. These terms are taken into account by the transformed Hamiltonian of eq. (23).

4.1 Mapped Hamiltonian

As we have already mentioned, the RPA method excludes in a first stage the H_{31} and H_{13} terms of the effective QCD Hamiltonian, eqs. (2)–(8). However, once the RPA method is implemented and their solutions known, the effective QCD Hamiltonian can be mapped onto a Hamiltonian that describes the propagation of the original fermionic particles (quarks and antiquarks) as well as the boson-like particles (ph, di-q and di-$\bar{q}$ phonons) and the interaction between them. The interaction terms between these particles correspond to the following step in this approximation on the description of the dynamics of effective particles at low-energy QCD. To write the explicit form of the vertex functions associated to these terms requires a larger space. For the sake of simplicity, in the present work we shall give a qualitative estimation of them. The procedure to get the vertex functions is rather straightforward: one needs to return to the effective Hamiltonian, eqs. (2)–(8), and replace the simple ph-pair, di-q and di-$\bar{q}$ operators by linear combinations of phonon operators. The latter is done by inverting eqs. (15), (16) and (17), where the pseudo-norm $X^2 - Y^2 = 1$ is satisfied by the forward and backward amplitudes of each phonon operator, as well as the relation between the forward and backward amplitudes, eq. (18).

The general form of the mapped effective Hamiltonian is given by

$$
\begin{aligned}
&H^{QCD}_{eff,\,map} = \\
&\sum_{\mathbf{q}\mu_q} \varepsilon_{\mathbf{q}} \left(\boldsymbol{b}^{\dagger}_{\mathbf{q}\mu_q} \boldsymbol{b}^{\mathbf{q}\mu_q} + \boldsymbol{d}^{\dagger}_{\bar{\mathbf{q}}\mu_q} \boldsymbol{d}^{\bar{\mathbf{q}}\mu_q} \right) \\
&+ \sum_{n} \sum_{\pi_n \gamma_n \mu_n} \omega_{n\pi_n\gamma_n} \boldsymbol{\Gamma}^{\dagger}_{n\pi_n,\gamma_n\mu_n} \boldsymbol{\Gamma}^{n\pi_n,\gamma_n\mu_n} \\
&+ \sum_{n\pi\gamma} \sum_{\mathbf{q}\mathbf{q}'} \Lambda^{(1)}_{n\pi\gamma;\mathbf{q}\mathbf{q}'} \sum_{\mu} \frac{(-1)^{\gamma-\mu}}{\sqrt{\dim(\gamma)}} \\
&\times \Big\{ \boldsymbol{\Gamma}^{\dagger}_{n=p\pi,\gamma\mu} \Big(\left[\boldsymbol{b}^{\dagger}_{\mathbf{q}} \otimes \boldsymbol{b}_{\bar{\mathbf{q}}'} \right]^{\bar{\gamma}}_{\bar{\mu}} \\
&+ (-1)^{\bar{\gamma}_{\mathbf{q}'} + \gamma_{\mathbf{q}} - \bar{\gamma}} \left[\boldsymbol{d}^{\dagger}_{\bar{\mathbf{q}}'} \otimes \boldsymbol{d}_{\mathbf{q}} \right]^{\bar{\gamma}}_{\bar{\mu}} \Big) + \text{h.c.} \Big\} \\
&+ \sum_{n\pi\gamma} \sum_{\mathbf{q}\mathbf{q}'} \Lambda^{(2)}_{n\pi\gamma;\mathbf{q}\mathbf{q}'} \sum_{\mu} \frac{(-1)^{\gamma-\mu}}{\sqrt{\dim(\gamma)}} \\
&\times \Big\{ \left(\boldsymbol{\Gamma}^{\dagger}_{n=a\pi,\gamma\mu} - (-1)^{\gamma-\mu} \boldsymbol{\Gamma}^{n=r\pi,\bar{\gamma}\bar{\mu}} \right) \left[\boldsymbol{d}^{\dagger}_{\bar{\mathbf{q}}} \otimes \boldsymbol{b}_{\bar{\mathbf{q}}'} \right]^{\bar{\gamma}}_{\bar{\mu}} \\
&+ \text{h.c.} \Big\}
\end{aligned}
$$

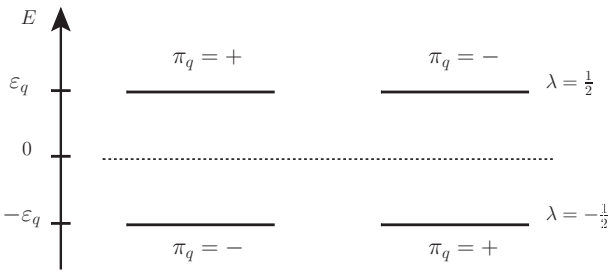

Fig. 1. Single-particle space of configurations. Each level (upper level for quarks ($\lambda = \frac{1}{2}$), lower level for antiquarks ($\lambda = -\frac{1}{2}$)) includes positive- and negative-parity states ($\pi_q = \pm$).

$$
\begin{aligned}
&+ \sum_{n\pi\gamma} \sum_{\mathbf{q}\mathbf{q}'} \Lambda^{(3)}_{n\pi\gamma;\mathbf{q}\mathbf{q}'} \sum_{\mu} \frac{(-1)^{\gamma-\mu}}{\sqrt{\dim(\gamma)}} \\
&\times \Big\{ \left(\boldsymbol{\Gamma}^{\dagger}_{n=a\pi,\gamma\mu} - (-1)^{\gamma-\mu} \boldsymbol{\Gamma}^{n=r\pi,\bar{\gamma}\bar{\mu}} \right) \left[\boldsymbol{b}^{\dagger}_{\mathbf{q}} \otimes \boldsymbol{d}_{\mathbf{q}'} \right]^{\bar{\gamma}}_{\bar{\mu}} + \text{h.c.} \Big\} .
\end{aligned}
\tag{23}
$$

For the interaction terms we have distinguished the type of phonon operator by the first index $n = p, a, r$, using the fact that $\gamma_r = \bar{\gamma}_a$ and understanding that the irreps γ, magnetic numbers μ and parity π of each phonon operator and the vertex coefficients must correspond to the phonon-type. In every interaction term the parity π associated with the corresponding phonon operator has to be equal to $\pi = \pi_q \times \pi_{q'}$, since the Hamiltonian is a scalar operator.

The quantities $\Lambda^{(i)}_{n\pi\gamma;\mathbf{q}\mathbf{q}'}$ are the vertex functions. Their expressions will be published elsewhere. In this contribution we will restrict severely the Hilbert space, in order to illustrate our procedure.

5 Effective interactions and numerical results

The calculation of the baryon-spectrum is a part of an extensive ongoing project [9,21,28–30]. Here we present a simple calculation to support the claim that a description of baryon states using many-body techniques and an effective Hamiltonian is feasible. As we mentioned before, the use of the interactions (23) needs to be further explained. The analysis involves *e.g.*, the renormalization of the vertex functions $\Lambda^{(i)}_{n\pi\gamma;\mathbf{q}\mathbf{q}'}$ in terms of the dimension of the space of configurations, similar to that presented in [9] for the renormalization of quark masses and interaction parameters. Therefore, to illustrate the method, we shall use effective vertex-coefficients $\Lambda^{(i)}_{n\pi\gamma;\mathbf{q}\mathbf{q}'} \to \Lambda^{(i)}$ and work in the minimal space of quark (antiquark) configurations depicted in fig. 1. The space of fig. 1 includes the lowest-energy state for quarks and antiquarks $\varepsilon_{\mathbf{q}}$ and $-\varepsilon_{\mathbf{q}}$, see table 2, which are obtained from the diagonalization of the kinetic term of eq. (6). The lowest RPA solutions for the ph-pair and di-q phonon states with energies $\omega_{n\pi_n\gamma_n}$ are shown in table 2.

It is worth adding a few words about the effective quark, ph- and di-q-phonon energies. The effective quark

Table 2. Quantum numbers ($T_n(J^{\pi_n}_n)$) and energies of the lowest effective quarks ($n = q$) and RPA phonon solutions for *ph*-pairs ($n = p$) and di-q ($n = a$), in units of [GeV]. The energy solutions for antiquark and phonon di-$\bar{q}$ are the same as those for the quark and phonon di-q respectively.

Effective particle	$T_n(J^{\pi_n}_n)$	Energy
quark	$\frac{1}{2}\left(\frac{1}{2}^{\pm}\right)$	$\varepsilon_q = 0.360$
ph-phonon	$1(0^-)$	$\omega_p = 0.705$
di-q-phonon	$0(0^+)$	$\omega_a = 1.131$

energy was set so that the mass of three effective quarks would be of the order of 1 GeV, which yields a harmonic oscillator length of 0.68 fm, while the energies of the *ph*- and di-q-phonon states were a consequence of using similar parameters to those used in [9]. However, since we are working in the minimal model space of fig. 1, some contributions are not considered for this calculation and their effects could modify the results shown in table 3. Some of these effects are already evident in the energies reported in table 2, like the effects of single-particle states with higher quantum numbers, *e.g.*, $N > 1$ and $J_q = \frac{3}{2}$. The inclusion of these states should affect both baryon states with $J_B = \frac{1}{2}, \frac{3}{2}$. In the case of higher oscillation quanta $N > 1$, the *ph*- and di-q-phonon states can acquire more and more collectivity due to the larger number of such pairs which can contribute to the vacuum of the model and generate lower energy phonon states. All of these effects and many others (like $l > 1$) will be considered in a further publication where an extended description of the baryon spectrum using many-body methods will be presented.

In here, within the subspace of fig. 1 and the phonon states of table 2, the baryon-like state for $J_B = \frac{1}{2}$ and $\frac{3}{2}$ can be written as

$$|T_B\,(J^{\pi_B}_B\rangle = b_1|B_1\rangle + b_2|B_2\rangle + b_3|B_3\rangle \qquad (24)$$

and

$$|T_B\,(J^{\pi_B}_B)\rangle = b'_1|B_1\rangle + b'_2|B_2\rangle, \qquad (25)$$

respectively. Thus, it is straightforward to show that in order to describe the transitions between the baryon-like states $|B_i\rangle$ of eqs. (19)–(21), the vertex-functions $\Lambda^{(1)}_{p\pi\gamma;\mathbf{qq}'}$ and $\Lambda^{(2)}_{a\pi\gamma;\mathbf{qq}'}$ contribute to the $T_B(J^{\pi_B}_B) = \frac{1}{2}(\frac{1}{2}^+)$ subspace and only $\Lambda^{(1)}_{p\pi\gamma;\mathbf{qq}'}$ to the $T_B(J^{\pi_B}_B) = \frac{3}{2}(\frac{3}{2}^+)$ subspace. Therefore, we will use three parameters in order to adjust the nucleon and Δ baryon energies up to 2 GeV. For the purpose of this numerical calculation we will only account for the colored components of the vacuum (01) and (10), by the di-quark and di-antiquark phonon operators, while for the *ph*-pair phonon operator we restrict to the colorless subspace (00).

In this example we restrict the dimensions to the minimal number of states described by the operators B_i of eqs. (19)–(21). For that purpose, we have removed the single-particle contributions to the baryon-like states $|B_i\rangle$ which have the same parity and energy, but higher angular momentum $\pi_q = (-1)^{\frac{1}{2}-\tau+l}$. For example, for the $|B_1\rangle$ states given by three quarks with total positive parity $\pi_{B_1} = \prod_{i=1}^{3}\pi_{q_i}$, there are two possibilities, one with the three effective quarks ($\lambda = \frac{1}{2}$) in the state with positive parity and the other with one quark with positive parity and two with negative parity. The latter is ignored in this calculation since the transformation of eq. (3), conserves parity in going from the harmonic-oscillator basis to the effective basis, but the negative-parity states come from angular-momentum excitations ($l = 1$). Applying the same criteria for the other B_i states, we have four B_1 states, six B_2 states and two B_3 states for $T_B(J^{\pi_B}_B) = \frac{1}{2}(\frac{1}{2}^+)$. Similarly, we have one B_1 state, three B_2 states and zero B_3 states for $T_B(J^{\pi_B}_B) = \frac{3}{2}(\frac{3}{2}^+)$. For the quantum numbers $T_B(J^{\pi_B}_B) = \frac{3}{2}(\frac{3}{2}^+)$, the B_3 states do not contribute as we have mentioned in sect. 3.4.

The parameters (*e.g.* values of the vertex functions Λ) used to calculate baryon-like states, and the resulting energies, are shown in table 3. The spectrum shows higher degeneracy around the states which are not affected by the interactions.

The parameters $\Lambda^{(i)}$ for the case $T_B(J^{\pi_B}_B) = \frac{1}{2}(\frac{1}{2}^+)$ were adjusted by fitting as close as possible, simultaneously, the energy E_1 to the proton energy and the E_4 state to the experimentally reported $N(1880)$ state, while the rest of the states are a consequence of such a fit. The results look promising, making the outstanding feature the contributions from the phonon states. In particular, the fact that the di-q-phonon state has a larger energy than the *ph*-phonon state and with it making possible to reach higher regions of the baryon spectrum. The larger energy of the di-q-phonon state was something theoretically expectable, since it represents a colored (confined) state and only acquiring physical meaning when couples to another colored object. As we have mentioned before, the phonon solutions (*ph* and di-q) will become more and more collective when the configuration space would be extended and with that at least one phonon state is to be expected at lower energies than those reported in table 2. The latter will generate improvements of the E_3 and E_5 solutions, needed for a better description of the $N(1710)$ and $N(2100)$ states, respectively.

The $N(1440)$ state or Roper resonance corresponds to a radial excitation of the nucleon. In simple quark models with a harmonic oscillator potential, where the nucleon is associated with the lowest state $N = 0$ and $l = 0$, the next positive-parity state, like the Roper resonance, corresponds to $N = 2$ and $l = 0$. However, experimentally the first negative-parity state $N(1535)$ which can be associated with $N = 1$ and $l = 1$ in quark models, turns out to be heavier than the Roper state and such parity reversal is not described correctly. In [31], the Roper resonance was described as a low-energy collective baryon excitation. Recently, the Roper resonance has had a theoretical well supported explanation [13], where its description as

Table 3. Vertex functions Λ, in units of MeV, and baryon energies E_i, in units of GeV, of states with quantum numbers $T_B(J_B^{\pi_B}) = \frac{1}{2}(\frac{1}{2}^+), \frac{3}{2}(\frac{3}{2}^+)$. The degeneration of each state is denoted by Ω_i.

$T_B(J_B^{\pi_B})$	$\Lambda^{(1)}$	$\Lambda^{(2)}$	$E_1(\Omega_1)$	$E_2(\Omega_2)$	$E_3(\Omega_3)$	$E_4(\Omega_4)$	$E_5(\Omega_5)$	$E_6(\Omega_6)$
$\frac{1}{2}\left(\frac{1}{2}^+\right)$	55	85	0.948(1)	1.080(3)	1.785(5)	1.862(1)	2.211(1)	2.266(1)
$\frac{3}{2}\left(\frac{3}{2}^+\right)$	106	–	1.035(1)	1.785(2)	1.830(1)	–	–	–

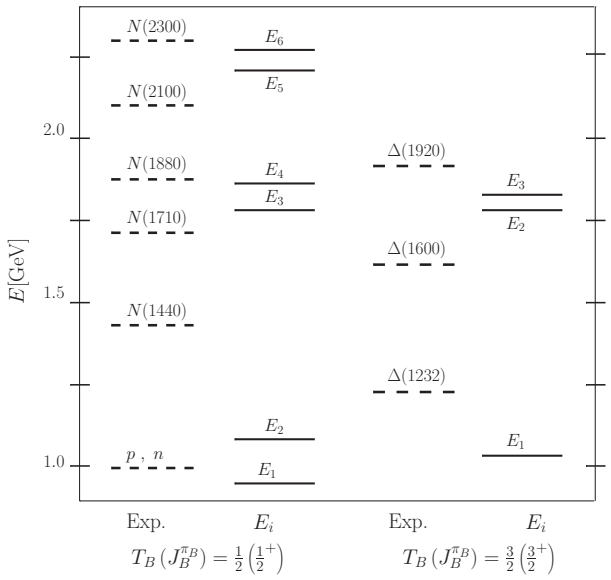

Fig. 2. Comparison between calculated energies E_i of baryon-like states (solid lines) with experimental values (dashed lines) taken from [32].

a proton's radial excitation has been corroborated and its low mass understood as an effect of a meson cloud that shields the quark core.

In the present work, the radial excitations $N > 1$ have not been considered in the configuration space of fig. 1. Thus, the low energy of the E_2 state concerning $N(1440)$ is understandable, since it represents basically three quarks without radial excitations. The radial excitations will be considered in a further publication as well as the influence of more collective meson-like states on the baryon-like spectrum, *i.e.*, the B_2 contributions. The latter will provide a closer description, in this model, of the Roper state as the one given in [13].

For the case of $T_B(J_B^{\pi_B}) = \frac{3}{2}(\frac{3}{2}^+)$, if the parameter $\Lambda^{(1)}$ is set to zero the model predicts one state at 1.080 GeV and another to 1.785 GeV, which it is a rough estimation for the observed experimental states $\frac{3}{2}(\frac{3}{2}^+)$ below 2 GeV, see fig. 2. In this case, it is evident that the physical $\Delta(1232)$ state is not well reproduced with three effective quarks, all of them with $J_q = \frac{1}{2}$, and being the first indicator that higher-energy contributions could be needed, *e.g.* higher harmonic-oscillator quanta $N > 1$ and single particle states with $J_q = \frac{3}{2}$. Once the interaction is turned on, the parameter $\Lambda^{(1)}$ is chosen such that the energy difference between the eigenvalue E_1 and the $\Delta(1232)$ state is not larger than 200 MeV, letting the highest eigenvalue be located at 1.830 GeV. The energy difference between the two higher solutions E_2 and E_3 is smaller than the observed between the $\Delta(1600)$ and the $\Delta(1920)$. In this case, the E_2 solution is expected to be improved with a larger configuration space, as mentioned before, but the E_1 solution seems to need single-particle contributions with $N > 1$ or $J_q = \frac{3}{2}$, which will rise the E_1 energy closer to the $\Delta(1232)$ state.

6 Conclusions

We have presented a description of baryon-like states within an effective QCD Hamiltonian, including only 4 orbitals states (two particle and two antiparticle states), which is simplistic but enabled us to understand the possible detailed structure of baryon-like states. The main conjecture is that colored pairs may contribute to the structure of these states by means of collective excitations and the resulting ground-state correlations. We started from the QCD Hamiltonian within the Coulomb Gauge and then applied several steps, as restricting to few orbitals states, leading to a coupling scheme of effective degrees of freedom. We applied the RPA method to deduce the spectrum of the baryon-like states. The results are quite encouraging, since they show that the use of non-perturbative many-body techniques, borrowed and adapted from more conventional many-body methods, are powerful enough to simplify the task of treating many quark and antiquark configurations within the real QCD, as needed for the microscopic interpretation of baryon states at low energy.

One of the authors (TY-M) thanks the National Research Council of Argentina (CONICET) for a post-doctoral scholarships. OC is a member of the scientific career of the CONICET. POH acknowledges financial help from DGAPA-PAPIIT (IN100315) and from CONACYT (Mexico, grant 251817). This work has been supported financially by the CONICET (PIP-282) and by the ANPCYT of Argentina.

In memoriam: Prof. Walter Greiner, to whom this article is dedicated, was a very particular person whose interests has been extremely broad, ranging from nuclear physics, particle physics, atomic physics and many more. He was one of the principal founders of the GSI, a laboratory for heavy ion physics near Darmstadt, Germany, and of the *Frankfurt Institute for Advanced Physics* (FIAS) at the University in Frankfurt am Main, Germany. Practically all heavy ion physicists originated in Frankfurt or visited it frequently. Prof. Greiner helped to develop this new field which is very active today. Theories initiated in Frankfurt are relevant in experimental facilities like Brookhaven CERN and GSI. One of the authors of the present article (POH) was one of Prof. Greiner's two-hundred PhD students and he is very thankful for the very broad education experienced under the leadership of Prof. Greiner. There are only few persons which imprinted their thinking and actions into the physics community and Prof. W. Greiner was certainly one of them.

Appendix A. Effective quarks and antiquarks operators

The rule to raise and lower indices are the following:

$$\begin{aligned}
&\boldsymbol{b}^{\dagger}_{k\pi,J_qC_q(Y_q,T_q),M_{J_q}M_{C_q}M_{T_q}} = \\
&(-1)^{\chi_{F_q}+\chi_{C_q}}(-1)^{J_q-M_{J_q}}\boldsymbol{b}^{\dagger}{}^{\,k\pi J_q\bar{C}_q(-Y_q,T_q),-M_{J_q}\bar{M}_{C_q}-M_{T_q}} \\
&\boldsymbol{b}^{k\pi,J_qC_q(Y_q,T_q),M_{J_q}M_{C_q}M_{T_q}} = \\
&(-1)^{\chi_{F_q}+\chi_{C_q}}(-1)^{J_q-M_{J_q}}\boldsymbol{b}_{k\pi J_q\bar{C}_q(-Y_q,T_q),-M_{J_q}\bar{M}_{C_q}-M_{T_q}},
\end{aligned} \tag{A.1}$$

and similarly,

$$\begin{aligned}
&\boldsymbol{d}^{\dagger\,k\pi,J_qC_q(Y_q,T_q),M_{J_q}M_{C_q}M_{T_q}} = \\
&(-1)^{\chi_{F_q}+\chi_{C_q}}(-1)^{J_q+M_{J_q}}\boldsymbol{d}^{\dagger}_{k\pi,J_q\bar{C}_q(-Y_q,T_q),-M_{J_q}\bar{M}_{C_q}-M_{T_q}} \\
&\boldsymbol{d}_{k\pi,J_qC_q(Y_q,T_q),M_{J_q}M_{C_q}M_{T_q}} = \\
&(-1)^{\chi_{F_q}+\chi_{C_q}}(-1)^{J_q+M_{J_q}}\boldsymbol{d}^{k\pi,J_q\bar{C}_q(-Y_q,T_q),-M_{J_q}\bar{M}_{C_q}-M_{T_q}}.
\end{aligned} \tag{A.2}$$

The phase $(-1)^{\chi_{F_q}}$ is equal to $(-1)^{\frac{1}{3}+\frac{Y_q}{2}+M_{T_q}}$ [27]. The equivalent notation holds for the color phase $(-1)^{\chi_{C_q}}$.

References

1. H. Reinhardt *et al.*, arXiv:1706.02702v1 [hep-th].
2. A.P. Szczepaniak, E. Swanson, Phys. Rev. D **65**, 025012 (2001).
3. C. Feuchter, H. Reinhardt, Phys. Rev. D **70**, 105021 (2004).
4. D.R. Campagnari, H. Reinhardt, Phys. Rev. D **82**, 105021 (2010).
5. M. Pak, H. Reinhardt, Phys. Rev. D **88**, 125021 (2013).
6. P. Vastag, H. Reinhardt, D. Campagnari, Phys. Rev. D **93**, 065003 (2016).
7. D.R. Campagnari, E. Ebadati, H. Reinhardt, P. Vastag, Phys. Rev. D **94**, 074027 (2016).
8. P. Bicudo, M. Cardoso, F.J. Llanes-Estrada, T.V. Cauteren, Phys. Rev. D **94**, 054006 (2016).
9. D.A. Amor-Quiroz, T. Yépez-Martínez, P.O. Hess, O. Civitarese, A. Weber, arXiv:1704.01947 [nucl-th].
10. QCDSF-UKQCD Collaboration (W. Bietenholz *et al.*), Phys. Rev. D **84**, 054509 (2011).
11. R.G. Edwards, J.J. Dudek, D.G. Richards, S.J. Wallace, Phys. Rev. D **84**, 074508 (2011).
12. A. Bashir, L. Chang, I.C. Cloët, B. El-Bennich, Y. Liu, C.D. Roberts, P.C. Tandy, Commun. Theor. Phys. **58**, 79 (2012).
13. N. Suzuki, B. Juliá-Díaz, H. Kamano, T.-S.H. Lee, A. Matsuyama, T. Sato, Phys. Rev. Lett. **104**, 042302 (2010).
14. J. Segovia, B. El-Bennich, E. Rojas, I.C. Cloët, C.D. Roberts, S. Xu, H. Zong, Phys. Rev. Lett. **115**, 171801 (2015).
15. G. Eichmann, H. Sanchis-Alepuz, R. Williams, R. Alkofer, C.S. Fischer, Prog. Part. Nucl. Phys. **91**, 1 (2016).
16. P. Ring, P. Schuck, *The Nuclear Many Body Problem* (Springer, Heidelberg, 1980).
17. N.H. Christ, T.D. Lee, Phys. Rev. D **22**, 939 (1980).
18. T.D. Lee, *Particle Physics and Introduction to Field Theory* (Harwood Academic Publishers, New York, 1981).
19. A. Szczepaniak, E.S. Swanson, C.R. Ji, S.R. Cotanch, Phys. Rev. Lett. **76**, 2011 (1996).
20. A.P. Szczepaniak, E.S. Swanson, Phys. Lett. B **577**, 61 (2003).
21. T. Yépez-Martínez, P.O. Hess, A.P. Szczepaniak, O. Civitarese, Phys. Rev. C **81**, 045204 (2010).
22. Jeff Greensite, Adam P. Szczepaniak, Phys. Rev. D **91**, 034503 (2015).
23. Jeff Greensite, Adam P. Szczepaniak, Phys. Rev. D **93**, 074506 (2016).
24. F.J. Llanes-Estrada, S.R. Cotanch, Nucl. Phys. A **697**, 303 (2002).
25. P. Guo, A.P. Szczepaniak, G. Galata, A. Vassallo, E. Santopinto, Phys. Rev. D **78**, 056003 (2008).
26. P. Guo, T. Yépez-Martínez, A.P. Szczepaniak, Phys. Rev. D **89**, 116005 (2014).
27. J. Escher, J.P. Draayer, J. Math. Phys. **39**, 5123 (1998).
28. T. Yépez-Martínez, O. Civitarese, P.O. Hess, Int. J. Mod. Phys. E **25**, 1650067 (2016).
29. T. Yépez-Martínez, O. Civitarese, P.O. Hess, Int. J. Mod. Phys. E **26**, 1750012 (2017).
30. T. Yépez-Martínez, O. Civitarese, P.O. Hess, arXiv:1708.04980 [nucl-th]
31. M.V. Nuñez, S.H. Lerma, P.O. Hess, S. Jesgarz, O. Civitarese, M. Reboiro, Phys. Rev. C **70**, 035208 (2004).
32. C. Patrignani *et al.* (Particle Data Group), Chin. Phys. C **40**, 100001 (2016).